Published in final edited form as:
Curr Biol. 2006 December 19; 16(24): 2406–2417.

Human Wapl Is a Cohesin-binding Protein that Promotes Sister Chromatid Resolution in Mitotic Prophase

Rita Gandhi, **Peter Gillespie**[1], and **Tatsuya Hirano**[*]
Cold Spring Harbor Laboratory, One Bungtown Road, P. O. Box 100, Cold Spring Harbor, NY 11724

Summary

Background—The linkage between duplicated chromosomes (sister chromatids) is established during S phase by the action of cohesin, a multisubunit complex conserved from yeast to humans. Most cohesin dissociates from chromosome arms when the cell enters mitotic prophase, leading to the formation of metaphase chromosomes with two cytologically discernible chromatids. This process is known as sister chromatid resolution. While two mitotic kinases have been implicated in this process, it remains unknown exactly how the cohesin-mediated linkage is destabilized at a mechanistic level.

Results—The wings apart-like (Wapl) protein was originally identified as a gene product that potentially regulates heterochromatin organization in *Drosophila melanogaster*. We show that the human ortholog of Wapl is a cohesin-binding protein that facilitates its timely release from chromosomes arms during prophase. Depletion of Wapl from HeLa cells causes transient accumulation of prometaphase-like cells with chromosomes that display poorly resolved sister chromatids with a high level of cohesin. Reduction of cohesin relieves the Wapl-depletion phenotype, and depletion of Wapl rescues premature sister separation observed in Sgo1-depleted or Esco2-depleted cells. Conversely, overexpression of Wapl causes premature separation of sister chromatids. Wapl physically associates with cohesin in HeLa cell nuclear extracts. Remarkably, *in vitro* reconstitution experiments demonstrate that Wapl forms a stoichiometric, ternary complex with two regulatory subunits of cohesin, implicating its non-catalytic function in inactivating cohesin's ability to interact with chromatin.

Conclusions—Wapl is a new regulator of sister chromatid resolution that promotes release of cohesin from chromosomes by directly interacting with its regulatory subunits.

Keywords

Cohesin; Sister Chromatid Cohesion; Prophase; Mitosis

Introduction

The faithful segregation of duplicated chromosomes into daughter cells is essential for the growth, development and survival of all organisms. Extensive studies during the past decade have demonstrated that two multisubunit complexes, cohesin and condensin, play central roles in regulating a series of structural conversions of chromosomes required for segregation [1,

*To whom correspondence should be addressed, Phone: 516-367-8370; Fax: 516-367-8815, E-mail: hirano@cshl.edu.
[1]Present address: Wellcome Trust Biocentre, University of Dundee, Dundee DD1 5EH, Scotland, UK.

Supplemental Data including Supplemental Figures, Experimental Procedures are available at http//www.current-biology.com/…

2]. Cohesin establishes the linkage between duplicated DNAs during S phase. Although this process is commonly called sister chromatid cohesion, such “chromatids” are not cytological discernible at this stage of the cell cycle because they are present as a non-random yet amorphous mass of chromatin within the cell nucleus. At the onset of mitosis, condensin associates with chromatin and converts it into a discrete set of rod-shaped structures. Concomitantly, most of cohesin dissociate from chromosome arms, and topoisomerase II removes entanglement between the sister DNAs. As a consequence of these mechanistically complex events, metaphase chromosomes are assembled, in each of which two sister chromatids juxtaposed along their lengths become visible microscopically [3]. This process, often referred to as sister chromatid resolution or condensation, is an essential prerequisite for the complete separation of sister chromatids that subsequently occurs at the onset of anaphase. Since any errors in this series of events potentially create aneuploidy, a hallmark of cancer [4,5], it is important to understand how they are tightly regulated at a mechanistic level.

Cohesin and condensin are structurally related protein complexes that contain distinct pairs of SMC (structural maintenance of chromosomes) proteins as their core subunits [1,2]. The loading mechanism of condensin is not fully understood although cdk1-dependent phosphorylation is likely to have a crucial role [6]. In vertebrate cells, the release of cohesin occurs at two different stages of mitosis through different mechanisms. Phosphorylation events are involved in the bulk dissociation of cohesin from chromosome arms during prophase, whereas proteolytic cleavage facilitates the final release of residual cohesin primarily enriched at centromeres in anaphase [7,8]. At least two mitotic kinases, polo-like kinase (Plk1 in humans or Plx1 in *Xenopus*) and aurora B, participate in the first stage of cohesin release in prophase [9,10]. Although it is most likely that the polo-like kinase directly phosphorylates cohesin subunits, it remains unknown mechanistically how such a modification might lead to dissociation of the cohesin complex from chromosomes, and how many other factors might be required for the dissociation reaction. Recent studies have also shown that additional factors, such as Sgo1/Mei-S332 and Bub1, play important roles in differential regulation of cohesin dynamics at chromosome arms and centromeres [11–14]. It should be mentioned that none of these regulatory factors or kinases, except another class of proteins known as Pds5 [15], display a stable interaction with the cohesin complex, which is composed of two SMC subunits (Smc1 and Smc3) and two non-SMC subunits (Scc1/Rad21 and Scc3/SA).

Drosophila Wapl (wings apart-like) was originally identified as a gene product regulating heterochromatin organization: its mutants show parallel sister chromatids with apparently loosened cohesion at their centromeres [16]. An independent study also identified *Drosophila* Wapl as a factor important for normal chromosome segregation [17]. It has been reported that expression of human Wapl is linked to cervical carcinogenesis and tumor progression, and that it has a character of oncoproteins [18]. Human Wapl has also been identified as a binding partner of the Epstein-Barr virus transformation-related protein EBNA2 [19]. Thus, despite recent accumulation of intriguing data, the molecular function of this class of proteins in chromosome dynamics or cell proliferation remains largely unknown.

In the current study, we show that human Wapl plays a crucial role in facilitating sister chromatid resolution during mitotic prophase. When Wapl is depleted from HeLa cells, transient accumulation of prometaphase-like cells is observed in which two sister chromatids are poorly resolved. In these chromosomes, a high level of cohesin is detected on the central axis where two sister chromatids were linked to each other. Conversely, overexpression of Wapl increases the frequency of premature sister separation. Double depletion experiments provide evidence that Wapl directly acts on cohesin to dissociate it from chromosomes. Consistently, Wapl is co-immunoprecipitated with a subpopulation of cohesin from HeLa cell nuclear extracts. Moreover, reconstitution experiments using recombinant subunits demonstrate that Wapl binds to the two regulatory subunits of cohesin (Scc1 and SA1) and

forms a stoichiometric, ternary complex. Our results suggest that Wapl is a new regulator of sister chromatid resolution that promotes cohesin release by directly interacting with its regulatory subunits.

Results

Cell Cycle Dynamics of Wapl in HeLa Cells

To characterize the structural and functional properties of Wapl in human cells, we prepared three different antibodies, one against its C-terminal synthetic peptide and two against non-overlapping N- and C-terminal recombinant fragments. As judged by immunoblotting against total lysates of HeLa and MCF7 cells, these antibodies recognized a single band with an apparent molecular weight of ~160 kDa (Figure 1A; also see Figure S1). To test whether the protein level of Wapl might change at specific stages of the cell cycle, we prepared lysates from HeLa cells synchronized by two different methods: double-thymidine block and release and nocodazole block and release (Figure 1B and 1C; Figure S2A and S2B for FACS analyzes). Immunoblotting analysis of cell lysates obtained by both methods showed that the total level of Wapl remained relatively constant throughout the cell cycle. To examine the cellular localization of Wapl, HeLa cells were fixed with formaldehyde and stained with an anti-Wapl antibody. We found that the Wapl signal was detectable within the nucleus during interphase, but distributed in the whole cell by prometaphase. The signal returned onto the chromatin by late telophase. When the staining was performed after pre-extraction with a nonionic detergent to remove soluble proteins (Figure 1D), the signal was retained in the nucleus during interphase and in late telophase, suggesting that Wapl is bound to chromatin. No specific signal of Wapl was detectable on chromosomes from prometaphase to anaphase under this condition or on chromosome spreads prepared after hypotonic treatment (data not shown). A biochemical fractionation of asynchronously growing cells (~95% in interphase) revealed that Wapl was detected almost exclusively in the chromatin-bound fraction (P3; Figure 1E, lane 4). The Wapl proteins recovered in this fraction were solubilized by treatment with micrococcal nuclease (data not shown). In contrast, when nocodazole-treated cells (~92% in mitosis) were fractionated, ~30% of Wapl were detected in the soluble cytoplasmic fractions (S2; Figure 1E, lane 6) and another ~30% were easily released from chromatin (S3, Figure 1E, lane 7). Thus, as judged by these criteria, Wapl is a nuclear protein whose cell cycle dynamics is highly reminiscent of that of cohesin (e. g., [20]).

Depletion of Wapl Causes a Delay in Prometaphase

Next we investigated the effect of depletion of Wapl from HeLa cells using small interfering RNAs (siRNAs). More than 80% of Wapl were depleted after either one or two rounds of transfection using two independent siRNAs specific to Wapl (Figure 2A; also see Figure S1). As judged by FACS analysis, only a slight increase in a G2+M population of cells was observed after Wapl depletion (Figure S2C). When chromosome spreads were prepared from Wapl-depleted cells after hypotonic treatment, however, we found that the chromosomes were much longer than typical metaphase chromosomes observed in control cells (Figure 2B). The resolution of sister chromatids was compromised with an appearance of parallel sister chromatids, as judged by their staining with an antibody to Smc2, the core subunit of condensins. Aurora B was less concentrated at centromeres in these chromosomes. We refer these chromosomes as to “prometaphase-like” chromosomes. The frequency of these elongated chromosomes was higher in Wapl-depleted cells than in control cells even after 3 h of colcemid treatment (Figure 2C). Two independent siRNAs produced essentially the same phenotype. We also found a higher frequency of mitotic cells positive for Mad2 and Bub1 staining on kinetochores in Wapl-depleted cells than in control cells (Figure 2D), suggesting a prometaphase delay in the former population of cells. It is most likely that poor resolution of chromosome arms leads to a delay in the maturation of sister kinetochores arranged into a back-

to-back orientation, which may in turn keep the spindle checkpoint active. The prometaphase-like chromosomes observed in the Wapl-depleted cells did not display no noticeable abnormality in the relative distribution of condensin I and condensin II [21](Figure S3).

To assess the effect of Wapl depletion on cell cycle progression, the protein was depleted from a synchronized population of HeLa cells. To this end, cells were treated with thymidine 8 h after siRNA transfection and incubated for another 15 h. The cells were then released from the single thymidine block, and cell lysates were prepared at time intervals and analyzed by immunoblotting. At the same time, the population of mitotic cells was evaluated by staining with an anti-phospho-H3 (at serine 10) antibody and DAPI. We found that entry into and progression through mitosis became slow when cells were treated with Wapl siRNA, as judged by a broad peak of the mitotic index (Figure 2E) and a delayed accumulation of cyclin B (Figure 2F). However, they eventually exited mitosis. While chromosomes segregated without any severe defects under this condition, multi-lobed nuclei were observed at a high frequency in the Wapl-depleted cells (~24%) than in the control cells (~5%) at 16 h after the release (data now shown). To get further insights into the potential role of Wapl in mitotic progression, we performed a nocodazole arrest and release experiment using control and Wapl-depleted cells. The two populations of the cells displayed little difference in the drop in the mitotic index (Figure 2G) or the kinetics of cyclin B degradation (Figure 2H), suggesting that progression from prometaphase through anaphase was not largely affected when the level of Wapl was reduced. Again, the Wapl-depleted cells managed to segregate chromosomes but exhibited a high frequency of multi-lobed nuclei 6–10 hr after the release. These results are consistent with the notion that depletion of Wapl causes a prometaphase delay but does not arrest the cell cycle in mitosis.

Wapl Depletion Produces Prometaphase-like Chromosomes with Poorly Resolved Sister Chromatids and a High Level of Cohesin

Two mitotic kinases, polo-like kinase and aurora B, have been implicated in cohesin release during mitotic prophase [9,10], and in fact simultaneous depletion of the two kinases from *Xenopus* egg extracts causes a severe defect in sister chromatid resolution [10]. To investigate the role of Wapl in chromosome morphogenesis in greater details, we prepared chromosome spreads from cells treated with Plk1, aurora B or Wapl siRNA. They were simultaneously stained with anti-topoisomerase II to visualize the chromatid axis and with anti-Smc1 to assess the amount of cohesin left on the chromosomes. Consistent with previous studies [22,23], sister chromatids were juxtaposed in parallel in Plk1-depleted and aurora B-depleted chromosomes, indicating an enhanced cohesion along chromosome arms (Figure 3A, the second and third rows). These chromosomes retained a higher level of cohesin on their arms compared to those produced in control cells (Figure 3A, the first row; note that the small amount of cohesin enriched on centromeric regions are not detectable under this condition; e. g., [23]). We found that Wapl-depleted chromosomes displayed the severest defect in sister chromatid resolution (Figure 3A, the fourth row). Remarkably, the Smc1 signal retained in these chromosomes was very focused and narrowly restricted on the central axis of a chromosome where two sister chromatids were linked to each other (see Figure 3B for close-ups). In contrast, the Smc1 signal was more diffuse and distributed evenly in the Plk1-depleted or aurora B-depleted chromosomes (Figure 3A and 3B).

Functional Interactions among Wapl, Cohesin and Cohesin Regulators

If the delay in sister chromatid resolution observed in Wapl-depleted cells was indeed due to a defect in cohesin release, such a phenotype would be suppressed by reducing the cellular level of cohesin. To test this idea, the cohesin subunit Scc1 and Wapl were depleted either individually or simultaneously from HeLa cells (Figure 4A), and chromosome spreads prepared from these cells were stained with anti-Smc2 and CREST (Figure 4B). A quantitation

of these analyses was summarized in Figure 4C. Under this condition, chromosomes with well resolved arms were observed in control cells (Figure 4B, the first row) whereas Wapl-depleted cells produced prometaphase-like chromosomes in which sister chromatids were more tightly paired along their entire lengths (Figure 4B, the third row). Remarkably, the resolution defect was relieved partially when Scc1 was depleted together with Wapl, producing chromosomes reminiscent of, if not identical to, those observed in control cells (Figure 4B, the fourth row). The suppression was obvious not only along chromosome arms (as judged by anti-Smc2 staining) but also at centromeric regions (as judged by CREST staining). Nonetheless, the double depletion of Scc1 and Wapl siRNAs did not cause complete separation of sister chromatids that was observed in cells depleted of Scc1 alone (Figure 4B, the second row). A most likely interpretation is that a low level of cohesin present in the cells treated with Wapl and Scc1 siRNAs supports cohesion because this population was more stably bound to chromosomes due to the loss of Wapl function. As judged by FACS analysis and mitotic indexes, depletion of Wapl also suppressed mitotic arrest that would otherwise be observed in Scc1-depleted cells (Figures 4C and S2C).

To further understand how Wapl might work in sister chromatid resolution, we have tested for its functional interactions with Sgo1 and Esco2, proteins implicated in the protection of centromeric cohesion [11–13] and the establishment of cohesion [24], respectively. Although single depletion of Sgo1 caused a defective phenotype characterized by premature chromatid separation as reported previously [11,25], we found that the phenotype was effectively suppressed when Wapl was simultaneously depleted with Sgo1 (Figure 4D). This observation was reminiscent of the previous report that ectopic expression of a non-phosphorylatable form of SA2 (a cohesin subunit) partially suppressed segregation defects in Sgo1 siRNA-treated cells [13]. We also found that depletion of Wapl suppressed premature separation observed in cells depleted of Esco2 [24](Figure 4E). Thus, Wapl apparently counteracts these cohesin regulators under this condition. These results are consistent with the idea that Wapl plays a role in destabilizing cohesion during mitotic prophase, possibly by facilitating cohesin release from chromosome arms.

Overexpression of Wapl Produces Cells Displaying Premature Sister Separation at a High Frequency

If depletion of Wapl prevents or slows down release of cohesin from chromosomes, its overexpression could induce its untimely dissociation, resulting in premature sister separation. To address this question, we transiently transfected 293T cells with a plasmid in which full-length Wapl cDNA is expressed under the control of the CMV promoter. After surveying different transfection conditions, we chose a condition in which the transfected cells expressed 2–4 fold more of Wapl than untransfected cells or transfected cells with an empty vector (Figure 5A). FACS analysis showed a slight elevation of G2/M population in cells transfected with Wapl cDNA (Figure S2D). As judged by immunofluorescence analysis, however, the Wapl cDNA-transfected cells displayed a number of abnormal mitotic figures, such as massive misalignments of chromosomes and multipolar spindles (Figure 5B and 5C). These defects were very similar to those observed in Scc1-depleted cells (Figure 4A-C). The distribution of Sgo1 on these abnormal mitotic cells was reminiscent of that found in cells treated with Scc1 siRNAs (R. G., unpublished results). Furthermore, a substantial population of the cells displaying abnormal chromosome arrangements (~70%) was positive for cyclin B staining, indicating that they did not undergo normal anaphase. Consistently, as judged by chromosome spread analyses, aberrantly separated sister chromatids were observed at a high frequency in the Wapl-overexpressing cells (Figure 5C and 5D), implicating the occurrence of premature sister separation before the onset of anaphase.

Wapl Associates with the Cohesin Complex in HeLa Cell Nuclear Extracts

The observation that Wapl was involved in the release of cohesin during early mitosis prompted us to test for their physical interactions. To this end, HeLa cell nuclear extracts were subjected to immunoprecipitations using control IgG and specific antibodies against Smc1 and Wapl. The immunoprecipitates were washed with a buffer containing 0.1 M or 0.5 M KCl, resolved by SDS-PAGE, and analyzed by silver staining (Figure 6A) and immunoblotting (Figure 6B). Anti-Smc1 precipitated cohesin subunits (Smc1, SA2 and Scc1) as well as Pds5A and Pds5B, as had been shown before [7, 15]. We found that Wapl was also readily detectable in the precipitate (Figure 6A&B, lane 3). The association of Wapl with cohesin was relatively tight as judged by its partial resistance to high-salt wash (Figure 6B, lane 4). Conversely, anti-Wapl precipitated not only Wapl itself, but also the cohesin subunits and Pds5A (Figure 6A&B, lanes 5 and 6). A less amount of Pds5B was detectable in these precipitates, suggesting that Wapl might bind preferentially, if not exclusively, to a subpopulation of cohesin associated with Pds5A. This was also confirmed by reciprocal immunoprecipitations with anti-Pds5A or anti-Pds5B (Figure 6C). On the other hand, we found no evidence that Wapl might preferentially associate with one of the two different populations of cohesin containing SA1 or SA2 (data not shown). As judged by the amount of proteins remaining in the extract after immunoprecipitations, we estimated that ~70% of Wapl associate with cohesin, whereas ~30–40% of cohesin associate with Wapl in a HeLa cell nuclear extract (data not shown). In fact, when the extract was subjected to sucrose gradient centrifugation, the majority of Wapl was co-fractionated with the major peak of cohesin (Figure 6D). These results suggest that Wapl associates tightly with a subpopulation of cohesin in HeLa cell nuclear extracts. Finally, we performed reciprocal immunoprecipitation using a salt-extracted chromatin fraction prepared from asynchronous cells and a soluble cytoplasmic fraction prepared from nocodazole-arrested cells. The interaction between Wapl and cohesin was detected in both fractions, and the relative ratios of the two components recovered in the precipitates were indistinguishable from each other (data not shown). Thus, it appears that Wapl associates with both chromatin-bound and soluble pools of cohesin.

In Vitro Reconstitution Reveals a Direct and Stoichiometric Interaction between Wapl and the Non-SMC Dimer of Cohesin

The co-immunoprecipitation experiments described above by no means addressed the question of whether Wapl might make a direct contact with a cohesin subunit(s). It was formally possible, for example, that the interaction between Wapl and cohesin is indirect and is mediated by a linker protein such as Pds5A. To clarify this problem, we attempted to reconstitute the interaction between Wapl and cohesin subunits by using recombinant proteins expressed with the aid of baculoviruses. The four subunits of the human cohesin complex (Smc1, Smc3, Scc1 and SA1) were co-expressed with Wapl in different combinations in insect cells. The cell lysates were subjected to immunoprecipitation reactions with appropriate antibodies, and the precipitates were fractionated by SDS-PAGE and analyzed by silver stain and immunoblotting. We found very little, if any, interaction between Wapl and the Smc1-Smc3 dimer (Figure 7A, lanes 4–6). Wapl associated only weakly with Smc1-Smc3-Scc1 (Figure 7A, lanes 7–9), but more efficiently with Smc1-Smc3-Scc1-SA1 (Figure 7A, lanes 10–13), indicating that the Wapl-cohesin interaction was mediated through the Scc1 and SA1 subunits. We then set up a similar reconstitution assay without the Smc1-Smc3 dimer. Wapl interacted only weakly with Scc1 alone, but not with SA1 alone (Figure 7B, lanes 4–7). Remarkably, however, we found that, when Wapl was co-expressed with Scc1 and SA1 together, the three proteins formed a very robust complex in a near-stoichiometric fashion (Figure 7B, lanes 8–10). These results strongly suggest that Wapl makes a direct contact to Scc1 and SA1 only when they associate with each other to form a non-SMC dimer. Finally, a series of binding assays using truncated versions of Wapl demonstrated that the N-terminal half of Wapl is primarily responsible for its binding to cohesin (Figure S4 and S5).

Discussion

Sister chromatid resolution is a process in which the linkage between two chromatids is partially dissolved from prophase through metaphase, and is thought to be a prerequisite for the complete and irreversible separation of sister chromatids that initiates at the onset of anaphase. In the current study, we report a new regulator of sister chromatid resolution, Wapl. Sister chromatid resolution is a mechanistically complex event, and its successful achievement requires not only bulk release of cohesin but also coordinated actions of condensin and topoisomerase II. Therefore, misregulation of condensin or topoisomerase II could, in principle, cause defects in sister chromatid resolution. Several lines of evidence strongly suggest, however, that Wapl directly regulates the dissociation of cohesin by physically interacting with its non-SMC components.

Depletion of Wapl from HeLa cells produces prometaphase cells having elongated chromosomes with poorly resolved sister chromatids at a high frequency. Although a transient delay is observed, the Wapl-depleted cells eventually enter metaphase and segregate chromosomes in anaphase. This apparently partial phenotype could be due to an incomplete depletion of Wapl from the cells under the condition tested. Alternatively, Wapl may associate with and regulate a subpopulation of cohesin distributed along chromosome arms. In fact, as judged by our estimation, only ~30–40% of cohesin associates with Wapl in HeLa cell nuclear extracts. Finally, the eventual segregation of incompletely resolved sister chromatids in Wapl-depleted cells could be achieved by separase-mediated cleavage of cohesin in anaphase, as has been implicated in cells defective in Plk1 and aurora B [23]. It should be added, however, that multi-lobed nuclei were frequently observed in the subsequent telophase, indicating that anaphase segregation (and/or subsequent reassembly of the nucleus) may not be completely normal in Wapl-depleted cells.

A series of double depletion and overexpression experiments reported here is also consistent with the idea that Wapl directly promotes cohesin's dissociation from chromosome arms during prophase. Reduction of the level of cohesin itself partially relieves the resolution defect observed in Wapl-depleted cells, and depletion of Wapl rescues premature separation of sister chromatids observed in cells depleted of cohesin regulators such as Sgo1 and Esco2. Conversely, overexpression of Wapl in 293T cells produces cells displaying premature sister separation at a high frequency. We also find that Sgo1 fails to be concentrated at centromeres and distributes along arms of the prometaphase-like chromosomes in Wapl-depleted cells (Figure S6), a phenotype reminiscent of, if not identical to, that observed in Bub1-depleted cells [11]. These observations support the existence of an intricate regulatory network of sister chromatid cohesion, in which cohesin's loading and unloading are tightly controlled both temporally and spatially [26].

Wapl was originally identified in *Drosophila* whose mutations cause loosened cohesion at centromeres [16]. At first glance, the phenotype observed in the *Drosophila* mutants is different from the defect observed in HeLa cells depleted of Wapl. However, the apparent defect in centromeric cohesion observed in the *Drosophila* mutants could be explained by enhanced arm cohesion because a tight balance between cohesion at centromeres and arms affects the shape of mitotic chromosomes (e. g. [23]). An implication of these observations is that Wapl may act primarily on chromosome arms, and not on centromeres. Consistent with this idea, we show that in HeLa cell nuclear extracts Wapl displays a high affinity for a subpopulation of cohesin containing Pds5A, a specific form of Pds5 proteins that has been predicted to have a role in arm cohesion [15]. In terms of phylogeny, we have so far been unable to find a Wapl ortholog in *Saccharomyces cerevisiae*. This may be consistent with the fact that the so-called prophase pathway of cohesin release is less prominent in this organism than in higher eukaryotes. The nematode *Ceanorhabditis elegans* has an ortholog (R08C7.10) whose depletion causes an

embryonic lethality [27,28]. The mouse *wapl* gene is also essential for embryonic development (cited in [18]). Functional characterization of these orthologs, in particular its relationship to sister chromatid resolution, needs to await future studies.

Previous biochemical analysis using yeast cohesin subunits showed that Scc1 links the Smc1-Smc3 dimer to Scc3 (the yeast ortholog of vertebrate SA1/SA2)[29]. Our reconstitution experiments reported here demonstrate that Wapl interacts directly with the holocomplex (Smc1-Smc3-Scc1-SA1), and even more robustly with the Scc1-SA1 dimer. Interestingly, Wapl associates poorly with Scc1 or SA1 alone, and does not bind to the Smc1-Smc3 dimer at all. Furthermore, no evidence is available for the occurrence of a free population of the Scc1-SA dimer in HeLa cell nuclear extracts [7]. Taken these results together, it is most likely that Wapl binds to a surface shared between Scc1 and SA1 only in the context of the holocomplex *in vivo* (Figure 7C). It is reasonable to speculate that Wapl uses this property to discriminate a functional population of cohesin (i.e., the holocomplex) from other intermediate assemblies (e. g., Smc1-Smc3-Scc1).

It remains to be determined mechanistically how Wapl might modulate the activity or conformation of cohesin and contribute to its dissociation from chromosomes. We have considered several potential mechanisms of action of Wapl. Firstly, Wapl may actively recruit protein kinases, implicated in cohesin dissociation such as Plk1, to cohesion sites during mitotic prophase [9,10]. This is an antagonistic role to the proposed action of Sgo1, which has recently shown to recruit protein phosphatase 2A to centromeric regions and to protect centromeric cohesion by maintaining a dephosphorylated state of cohesin [30–32]. Secondly, a near-stoichiometric binding between Wapl and the Scc1-SA1 dimer may suggest a more active, non-catalytic role in inducing conformational changes of cohesin that eventually leads to its dissociation from chromatin. Alternatively, Wapl may have a role in preventing a dissociated population of cohesin from rebinding to chromatin rather than participating in an active dissociation reaction. For example, when the linkage between the Scc1-SA dimer and one of the SMC subunits is disrupted during the dissociation reaction, Wapl could bind to and sequester the liberated end of the Scc1-SA dimer and thereby prevent the cohesin ring from being closed again (Figure 7C). The apparent difference in Wapl's affinity for the holocomplex and the Scc1-SA1 dimer, as revealed by the reconstitution assay, may be consistent with this idea. Of course, these models are not mutually exclusive from each other. Whatever the mechanisms might be, it is clear that Wapl is a unique class of cohesin regulators that may directly destabilize the interaction between cohesin and chromatin.

High-level expression of human Wapl was observed in cervical cancers, and 3T3 cells overexpressing Wapl developed tumors when injected into nude mice [18]. Our current results show that overexpression of Wapl causes premature sister separation at a high frequency in 293T cells. One of the potential consequences of premature sister separation is the production of aneuploidy, a hallmark of many types of cancer [5]. Furthermore, accumulating lines of evidence suggest that misregulation of cohesin might cause developmental diseases in humans [33,34]. Therefore, further functional and mechanistic characterization of Wapl will undoubtedly enhance our understanding of how genome stability and expression are controlled through an elaborate mechanism that modulates cohesin dynamics and mobilization in the cell.

Experimental Procedures

Antibodies

Human Wapl was predicted to be a 1,190 amino-acid polypeptide (accession # NM_015045) with a calculated molecular mass of 133 kDa [18]. Rabbit polyclonal antisera were raised against a synthetic peptide corresponding to the C-terminal sequence of Wapl (GQKSISRVIEYLEH) and against N-terminal (amino acid #1–319) and C-terminal (#844–

1190) recombinant fragments of Wapl. We also prepared peptide antibodies against human Scc1/Rad21 (YSDIIATPGPRFHII) and human Smc1 (DLTKYPDANPNPNEQ), and antibodies against a recombinant fragment of human Sgo1 (accession # AAH01339/ NP_612493; amino acid #1–266). Characterization of the anti-Sgo1 antibody was described in Figure S7. All recombinant proteins were expressed from pRSET vectors (Invitrogen) in *Escherichia coli* as hexahistidine(his6)-fusions. Soluble proteins were purified on a Ni-NTA metal-affinity column (Qiagen), whereas insoluble proteins were purified by electroelution following SDS-PAGE. Antisera were affinity-purified on Affi-Gel (BioRad) coupled with peptides or recombinant protein as described previously [6]. Other rabbit polyclonal antibodies used in this study were: anti-Smc3, -SA1 and -SA2 [7,20]; anti-hCAP-E/Smc2 [35]; anti-Pds5A and -Pds5B [15]. We also used antibodies from commercial sources: anti-human aurora B (AIM-1, BD Biosciences); anti-α-tubulin (clone DM1A, Sigma); anti-Bub1 (K0168-3, MBL); anti-Bub1 (BL1680, Bethyl laboratories); anti-human cyclin B1 (Sc-245, Santa Cruz Biotechnology); anti-human Mad2 (BabCO); anti-Plk1 (Sc-17783, Santa Cruz Biotechnology); anti-human Topo IIα (monoclonal, TopoGEN). An anti-Esco2 antibody and a CREST serum were generously provided by H. Zou [24] and Y. Muro [36], respectively.

Cell Cultures and Small Interfering RNA (siRNA) Transfection

Asynchronously growing HeLa cells were maintained in Dulbecco's modified Eagle's medium supplemented with 10% fetal bovine serum and penicillin/streptomycin. Whenever required, nocodazole was added at a final concentration of 0.1 μg/ml 16 h before harvesting mitotic cells by shake off. Cells were transfected with 100 nM oligo siRNA duplexes (Dharmacon) using oligofectamine (Invitrogen) at 24 and 48 h after seeding [37]. Control cells were transfected with a transfection mixture containing no siRNAs. HeLa cells were synchronized at G1/S phase by double thymidine block using 2.5 mM thymidine [38]. For the synchronization experiments shown in Figure 2, cells were analyzed after release from single thymidine block. The sequence of the sense strand of the siRNA duplexes were: Wapl#1: CGGACUACCCUUAGCACAAdTdT; Wapl#2: CGAGCAGGAGACUGGUUUAdTdT; Plk1: GGGCGGCUUUGCCAAGUGCdTdT; Sgo1#1: ACAGUAGAACCUGCUCAGAdTdT; Sgo1#2: GUGAGCCUCUGUGAAUCAAdTdT; Scc1#1: AUACCUUCUUGCAGACUGUdTdT; Bub1: CCAGUGAGUUCCUAUCCAAdTdT; Esco2#1: UAAGUCCACUGUCUAUCCAdTdT; Esco2#2: GCAUCUUCAGUCAAUUCAAdTdT; Aurora B: GAGCCUGUCACCCCAUCUGdTdT. For overexperssion of Wapl, full-length Wapl cDNA was cloned in pcDNA3.1(+) and used to transiently transfect 293T cells using FuGene 6 (Roche) according to manufacturer's instructions. An initial optimization was performed by using different amounts of the plasmid and transfection reagent. The cells were transfected at ~50% confluency in a 6-well dish, and analyzed 42 h after transfection by immunoblotting and immunofluorescence analysis.

Immunofluorescence

For immunofluorescence, cells were seeded on 24-well plates containing poly-L-lysine coated coverslips. Alternatively, cells transfected in 6-well plates were trypsinized and an aliquot was spun on poly-L-lysine coated coverslip in cytospin (Thermo Shandon). The cells were fixed with 2% paraformaldehyde in 1x phosphate-buffered saline (PBS, pH 7.4) at room temperature for 15 min and then permeabilized in 0.5% Triton X-100 in PBS for 5 min. All steps were performed essentially as described before [21,22]. In some experiments, cells were pre-extracted in CSK buffer (10 mM PIPES [pH 7.0], 100 mM NaCl, 3 mM $MgCl_2$ and 300 mM sucrose) with 0.5% Triton X-100 at 4 °C for 5 min before fixation with 2% paraformaldehyde. Images were acquired using an Axioskop microscope (Carl Zeiss, Jena, Germany) equipped with a cooled charge-coupled device camera. Grayscale images were pseudocolored and

merged using Adobe Photoshop. When the phenotypes were quantified, more than 500 cells or approximately 100 chromosome spreads were analyzed.

Extract Preparation and Immunoprecipitations

For immunoblotting analysis of total lysates, $1x10^5$ cells were resuspended in 50 μl 1 x SDS sample buffer, heat-denatured for 2 min, and briefly sonicated. An aliquot of 10–20 μl was resolved by SDS-PAGE, and analyzed by immunoblotting. For immunoprecipitation from total cell extracts, cells were resuspended in a lysis buffer (50 mM Tris-HCl [pH 7.2], 250 mM NaCl, 0.1% NP-40, 2 mM EDTA, 10% glycerol, 40 mM β-glycerophosphate, 0.5 mM PMSF, 10 μg/ml each of leupeptin, chymostatin and pepstatin A) at a concentration of $2.5x10^7$ cells/ml, incubated at 4 °C for 30 min, sonicated briefly, and centrifuged at 12,000 rpm in a microfuge for 10 min. The clarified lysate was diluted with no salt buffer to reduce the salt concentration to 150 mM and was centrifuged again before using for immunoprecipitations. HeLa nuclear extracts were prepared in buffer B as described previously [7]. For immunoprecipitations, 5 μg of an affinity-purified antibody were added to 100 μl of nuclear extracts or 200 μl of total cell extracts, and incubated on ice for 1 h. Immunoprecipitates were recovered on 10 μl of protein A agarose beads (Invitrogen), washed several times with buffer B and analyzed by silver staining or immunoblotting. Biochemical fractionation of cell lysates was performed as described in [39].

Baculovirus-mediated Protein Expression

Full-length cDNAs encoding human cohesin subunits (hSmc1, hSmc3, hScc1, hSA1) and human Wapl were subcloned into pFASTBac (Invitrogen). The sources of the cDNA clones and the details of plasmid construction are described in Supplemental Data. The Bac-to-Bac baculovirus expression system (Invitrogen) was used to produce recombinant viruses according to the manufacturer's instruction. To express recombinant proteins, Sf9 cells were infected with the corresponding baculoviruses at a multiplicity of infection (M.O.I.) of ~1–5 and incubated at 27°C for 48 h. For immunoprecipitation experiments, ~3 $x10^6$ cells were resuspended in 0.5 ml of buffer L (20 mM Hepes [pH 7.7], 100 mM KCl, 2.5 mM $MgCl_2$, 0.1% Triton X-100, 10% glycerol, 10 μg/ml each of leupeptin, chymostatin and pepstatin A), and lysed by sonication. The lysate was frozen in liquid nitrogen in aliquots and stored at −80°C. Before immunoprecipitation, the lysate was thawed and centrifuged at 12,000 rpm for 10 min at 4°C.

Supplemental Data

Refer to Web version on PubMed Central for supplementary material.

Acknowledgements

We thank Ana Losada, Takao Ono and Michiko Hirano for technical suggestions and discussions, and K. Shintomi for help with baculovirus expression. We are grateful to Pamela Moody and Stephen Hearn for help with FACS analyses and microscopy. We also thank H. Zou, Y. Muro and M. Kuroda for providing anti-Esco2 antibody, CREST serum, and Wapl cDNA and anti-Wapl serum, respectively. Members of the Hirano lab provided critical comments on the manuscript. R.G. thanks Amitabh Mohanty for his comments on the manuscript. This work was supported by a grant from the National Institutes of Health (to T. H.).

References

1. Losada A, Hirano T. Dynamic molecular linkers of the genome: the first decade of SMC proteins. Genes Dev 2005;19:1269–1287. [PubMed: 15937217]
2. Nasmyth K, Haering CH. The structure and function of SMC and kleisin complexes. Annu Rev Biochem 2005;74:595–648. [PubMed: 15952899]

3. Hirano T. Chromosome cohesion, condensation and separation. Annu Rev Biochem 2000;69:115–144. [PubMed: 10966455]
4. Rajagopalan H, Lengauer C. Aneuploidy and cancer. Nature 2004;432:338–341. [PubMed: 15549096]
5. Draviam VM, Xie S, Sorger PK. Chromosome segregation and genomic stability. Curr Opin Genet Dev 2004;14:120–125. [PubMed: 15196457]
6. Hirano T, Kobayashi R, Hirano M. Condensins, chromosome condensation protein complexes containing XCAP-C, XCAP-E and a Xenopus homolog of the Drosophila Barren protein. Cell 1997;89:511–521. [PubMed: 9160743]
7. Losada A, Yokochi T, Kobayashi R, Hirano T. Identification and characterization of SA/Scc3p subunits in the Xenopus and human cohesin complexes. J Cell Biol 2000;150:405–416. [PubMed: 10931856]
8. Waizenegger IC, Hauf S, Meinke A, Peters JM. Two distinct pathways remove mammalian cohesin from chromosome arms in prophase and from centromeres in anaphase. Cell 2000;103:399–410. [PubMed: 11081627]
9. Sumara I, Vorlaufer E, Stukenberg PT, Kelm O, Redermann N, Nigg EA, Peters JM. The dissociation of cohesin from chromosomes in prophase is regulated by Polo-like kinase. Mol Cell 2002;9:515–525. [PubMed: 11931760]
10. Losada A, Hirano M, Hirano T. Cohesin release is required for sister chromatid resolution, but not for condensin-mediated compaction, at the onset of mitosis. Genes Dev 2002;16:3004–3016. [PubMed: 12464631]
11. Kitajima TS, Hauf S, Ohsugi M, Yamamoto T, Watanabe Y. Human Bub1 defines the persistent cohesion site along the mitotic chromosome by affecting shugoshin localization. Curr Biol 2005;15:353–359. [PubMed: 15723797]
12. Tang ZYS, Harley SE, Zou H, Yu H. Human Bub1 protects centromeric sister-chromatid cohesion through Shugoshin during mitosis. Proc Natl Acad Sci USA 2004;101:18012–18017. [PubMed: 15604152]
13. McGuinness B, Hirota T, Kudo NR, Peters JM, Nasmyth K. Shugoshin prevents dissociation of cohesin from centromeres during mitosis in vertebrate cells. PLoS Biol 2005;3:e86. [PubMed: 15737064]
14. Clarke AS, Tang TT, Ooi DL, Orr-Weaver TL. POLO kinase regulates the Drosophila centromere cohesion protein Mei-S332. Dev Cell 2005;8:53–64. [PubMed: 15621529]
15. Losada A, Yokochi T, Hirano T. Functional contribution of Pds5 to cohesin-mediated cohesion in human cells and Xenopus egg extracts. J Cell Sci 2005;118:2133–2141. [PubMed: 15855230]
16. Verni F, Gandhi R, Goldberg ML, Gatti M. Genetic and molecular analysis of wings apart-like (wapl), a gene controlling heterochromatin organization in Drosophila melanogaster. Genetics 2000;154:1693–1710. [PubMed: 10747063]
17. Dobie KE, Kennedy CD, Velasco VM, McGrath TL, Weko J, Patterson RW, Karpen GH. Identification of chromosome inheritance modifiers in Drosophila melanogaster. Genetics 2001;157:1623–1637. [PubMed: 11290718]
18. Oikawa K, Ohbayashi T, Kiyono T, Nishi H, Isaka K, Umezawa A, Kuroda M, Mukai K. Expression of a novel human gene, human wings apart-like (hWAPL) is associated with cervical carninogenesis and tumor progression. Cancer Res 2004;64:3545–3549. [PubMed: 15150110]
19. Kwiatkowski BA, Ragoczy T, Ehly J, Schubach WH. Identification and cloning of a novel chromatin-associated protein partner of Epstein-Barr nuclear protein 2. Exp Cell Res 2004;300:223–233. [PubMed: 15383329]
20. Losada A, Hirano M, Hirano T. Identification of Xenopus SMC protein complexes required for sister chromatid cohesion. Genes Dev 1998;12:1986–1997. [PubMed: 9649503]
21. Ono T, Losada A, Hirano M, Myers MP, Neuwald AF, Hirano T. Differential contributions of condensin I and condensin II to mitotic chromosome architecture in vertebrate cells. Cell 2003;115:109–121. [PubMed: 14532007]
22. Ono T, Fang Y, Spector D, Hirano T. Spatial and temporal regulation of condensins I and II in mitotic chromosome assembly in human cells. Mol Biol Cell 2004;15:3296–3308. [PubMed: 15146063]
23. Gimenez-Abian JF, Sumara I, Hirota T, Hauf S, Gerlich D, De la Torre C, Ellenberg J, Peters JM. Regulation of sister chromatid cohesion between chromosome arms. Curr Biol 2004;14:1187–1193. [PubMed: 15242616]

24. Hou F, Zou H. Two human orthologues of Eco1/Ctf7 acetyltransferases are both required for proper sister-chromatid cohesion. Mol Biol Cell 2005;16:3908–3918. [PubMed: 15958495]
25. Salic A, Waters JC, Mitchison TJ. Vertebrate shugoshin links sister centromere cohesion and kinetochore microtubule stability in mitosis. Cell 2004;118:567–578. [PubMed: 15339662]
26. Watanabe Y. Sister chromatid cohesion along arms and at centromeres. Trends Genet 2005;21:405–412. [PubMed: 15946764]
27. Kamath RS, Fraser AG, Dong Y, Poulin G, Durbin R, Gotta M, Kanapin A, Le Bot N, Moreno S, Sohrmann M, Welchman DP, Zipperlen P, Ahringer J. Systematic functional analysis of the Caenorhabditis elegans genome using RNAi. Nature 2003;421:231–237. [PubMed: 12529635]
28. Simmer F, Moorman C, van der Linden AM, Kuijk E, van den Berghe PV, Kamath RS, Fraser AG, Ahringer J, Plasterk RH. Genome-wide RNAi of C. elegans using the hypersensitive rrf-3 strain reveals novel gene functions. PLoS Biol 2003;1:E12. [PubMed: 14551910]
29. Haering CH, Lowe J, Hochwagen A, Nasmyth K. Molecular architecture of SMC proteins and the yeast cohesin complex. Mol Cell 2002;9:773–788. [PubMed: 11983169]
30. Kitajima TS, Sakuno T, Ishiguro K, Iemura S, Natsume T, Kawashima SA, Watanabe Y. Shugoshin collaborates with protein phosphatase 2A to protect cohesin. Nature 2006;441:46–52. [PubMed: 16541025]
31. Riedel CG, Katis VL, Katou Y, Mori S, Itoh T, Helmhart W, Galova M, Petronczki M, Gregan J, Cetin B, Mudrak I, Ogris E, Mechtler K, Pelletier L, Buchholz F, Shirahige K, Nasmyth K. Protein phosphatase 2A protects centromeric sister chromatid cohesion during meiosis I. Nature 2006;441:53–61. [PubMed: 16541024]
32. Tang Z, Shu H, Qi W, Mahmood NA, Mumby MC, Yu H. PP2A is required for centromeric localization of Sgo1 and proper chromosome segregation. Dev Cell 2006;10:575–585. [PubMed: 16580887]
33. Strachan T. Cornelia de Lange Syndrome and the link between chromosomal function, DNA repair and developmental gene regulation. Curr Opin Genet Dev 2005;15:258–264. [PubMed: 15917200]
34. Dorsett D. Roles of the sister chromatid cohesion apparatus in gene expression, development, and human syndromes. Chromosoma. 2006in press
35. Kimura K, Cuvier O, Hirano T. Chromosome condensation by a human condensin complex in Xenopus egg extracts. J Biol Chem 2001;276:5417–5420. [PubMed: 11136719]
36. Muro Y, Sugimoto K, Okazaki T, Ohashi M. The heterogeneity of anti-centromere antibodies in immunoblotting analysis. J Rheumatol 1990;17:1042–1047. [PubMed: 2213779]
37. Elbashir SM, Harborth J, Lendeckel W, Yalcin A, Weber K, Tuschl T. Duplexes of 21-nucleotide RNAs mediate RNA interference in cultured mammalian cells. Nature 2001;411:494–498. [PubMed: 11373684]
38. Jallepalli PV, Waizenegger IC, Bunz F, Langer S, Speicher MR, Peters JM, Kinzler KW, Vogelstein B, Lengauer C. Securin is required for chromosomal stability in human cells. Cell 2001;105:445–457. [PubMed: 11371342]
39. Mendez J, Stillman B. Chromatin association of human ORC, Cdc6 and MCM proteins during the cell cycle: assembly of pre-replication complexes in late mitosis. Mol Cell Biol 2000;20:8602–8612. [PubMed: 11046155]

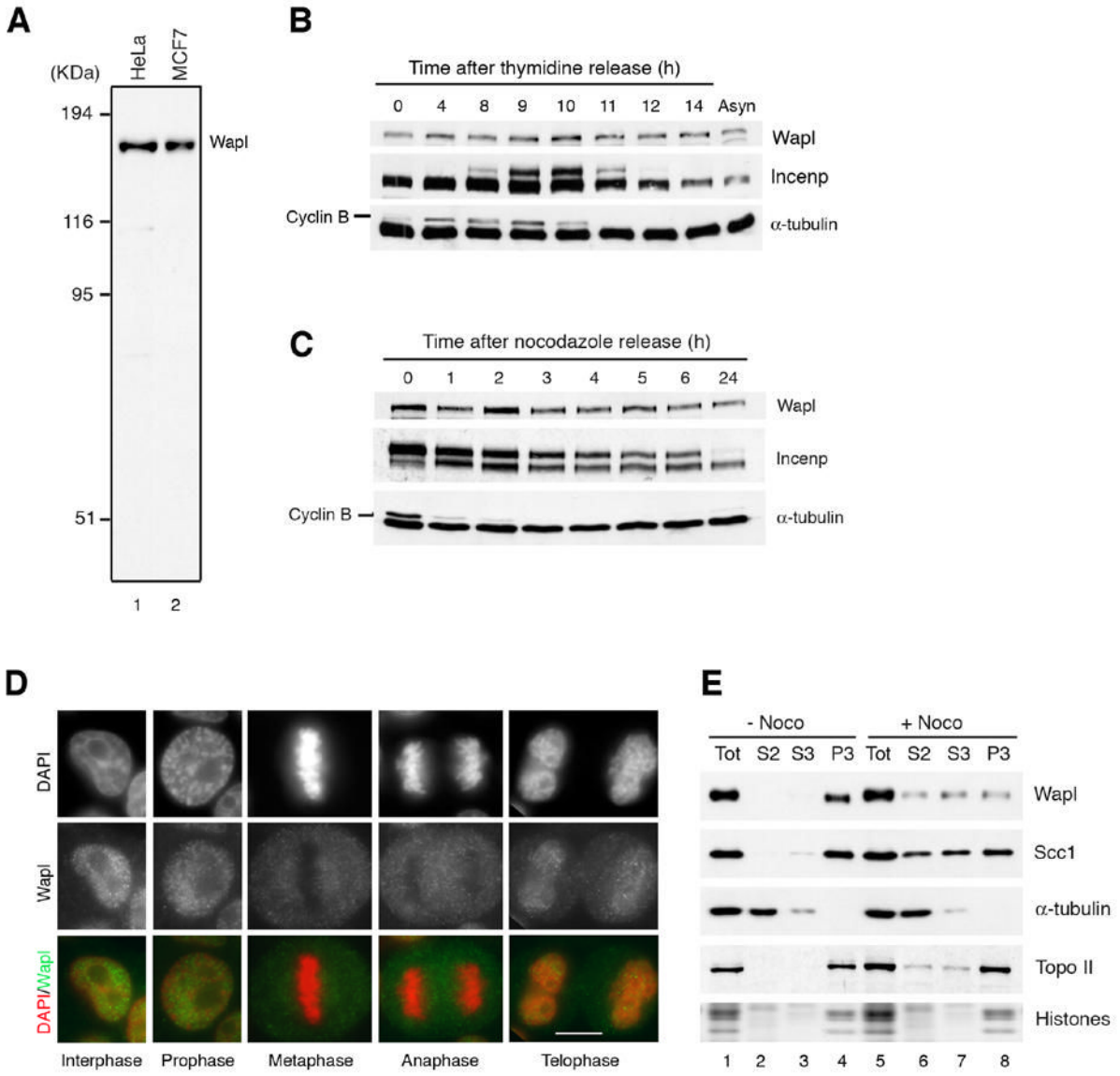

Figure 1.

Cell Cycle Dynamics of Wapl in HeLa Cells. (A) Total cell lysates were prepared from HeLa cells (lane 1) and MCF7 cells (lane 2), and analyzed by immunoblotting with an antibody against an N-terminal recombinant fragment of Wapl. (B) HeLa cells were synchronized by means of double-thymidine block and release. Total cell lysates were prepared at time intervals, and analyzed by immunoblotting with the antibodies indicated. Mitosis-specific mobility shift of Incenp and the level of cyclin B were used as markers to monitor cell cycle progression. α-tubulin was used as a loading control. The final lane contains a lysate prepared from an asynchronous culture (Asyn). (C) HeLa cells were arrested in mitosis with nocodazole for 16 h and then released. Total cell lysates were prepared at time intervals, and analyzed as above. (D) HeLa cells were pre-extracted with a buffer containing 0.5% Triton X-100, fixed with paraformaldehyde, and stained with anti-Wapl and DAPI. Bar, 10 μm. (E) Cell lysates were prepared from asynchronously growing HeLa cells (-Noco) and from HeLa cells treated with nocodazole for 16 hr (+Noco). The total cell lysates (lanes 1 and 5) were separated into soluble cytoplasmic fraction (S2, lanes 2 and 6), soluble nucleoplasmic fraction (S3, lanes 3 and 7)

and chromatin-enriched fractions (P3, lanes 4 and 8), and they were analyzed by immunoblotting with the indicated antibodies (top four rows). The lowest row represents the level of histones recovered in each lane, which were visualized by Coomassie blue stain.

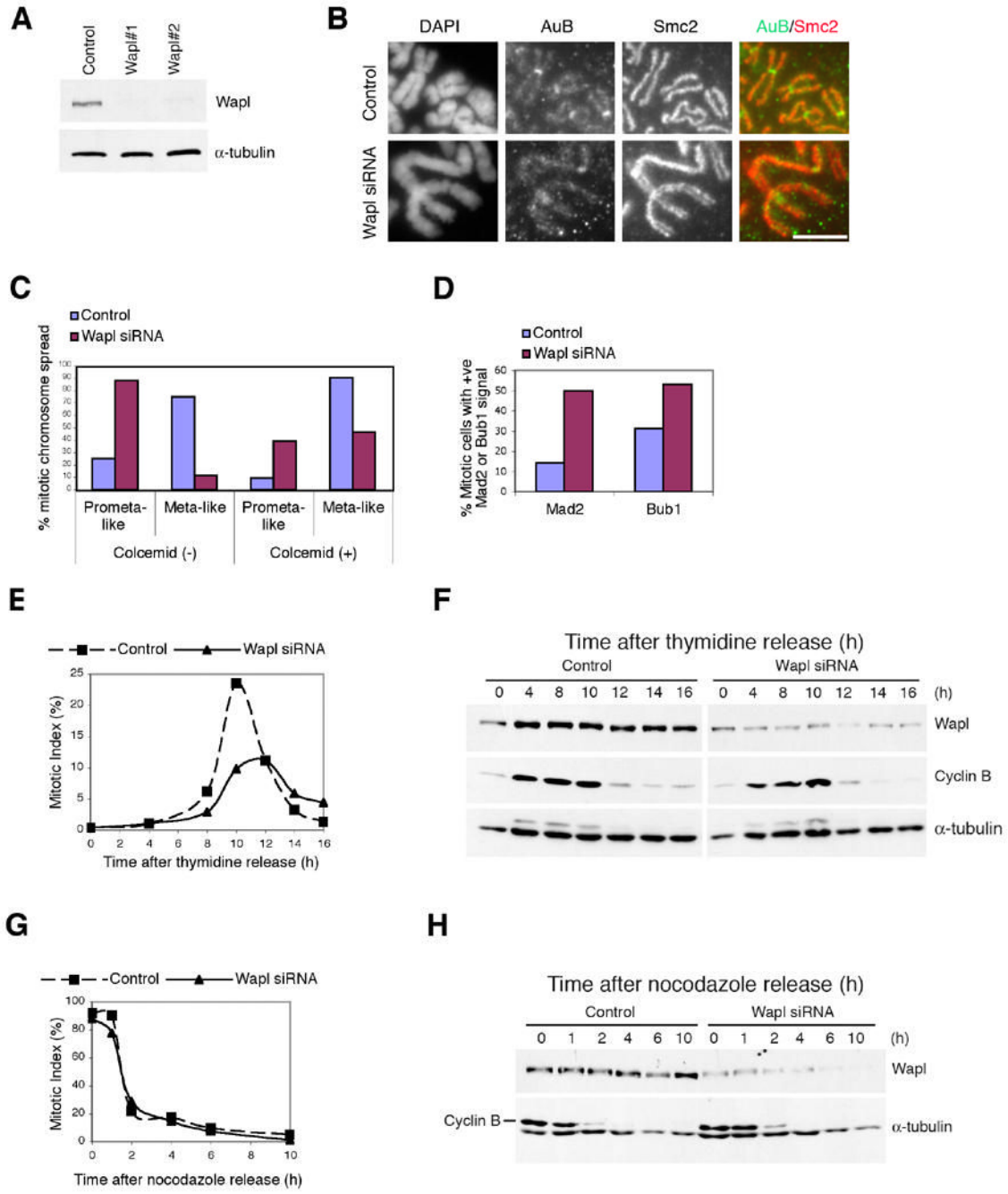

Figure 2.

Depletion of Wapl Produces an Increased Population of Prometaphase Cells. (A) HeLa cells were transfected with two independent Wapl siRNAs and analyzed for protein levels by immunoblotting. Mock-transfected cells without siRNAs served as controls. (B) Chromosome spreads were prepared (without colcemid treatment) from the control and Wapl-depleted cells after hypotonic treatment, and stained with anti-aurora B (AuB) and anti-Smc2 (left panels). Bar, 5 μm. (C) The mitotic figures on the spreads were classified into “prometaphase-like” (B, lower panels) and “metaphase-like” (B, upper panels), and their numbers are plotted (Colcemid -). Chromosome spreads were also prepared from cells treated with colcemid for 3 hr, and analyzed similarly (Colcemid +). (D) The control and Wapl-depleted cells were fixed and

stained with anti-Mad2 or anti-Bub1. The frequency of mitotic cells positive for Mad2 and Bub1 was plotted. (E) HeLa cells were treated with thymidine 8 h after mock-transfection (control) or Wapl siRNA transfection, incubated for another 15 h, and then released from the thymidine block. The frequency of mitotic cells was assessed by staining with anti-phospho-H3 (at serine 10) and DAPI. (F) In the same experiments as described in (E), cell lysates were prepared at the indicated time points, and analyzed by immunoblotting. The upper faint band in the third row (α-tubulin) is cyclin B signal as the blot was first probed with cyclin B and then with α-tubulin without stripping. (G) and (H) HeLa cells were mock-transfected (control) or transfected with Wapl siRNA, incubated for 24 h, and treated with nocodazole for 16 h. After release from the nocodazole arrest, the cells were analyzed as in (E) and (F), respectively.

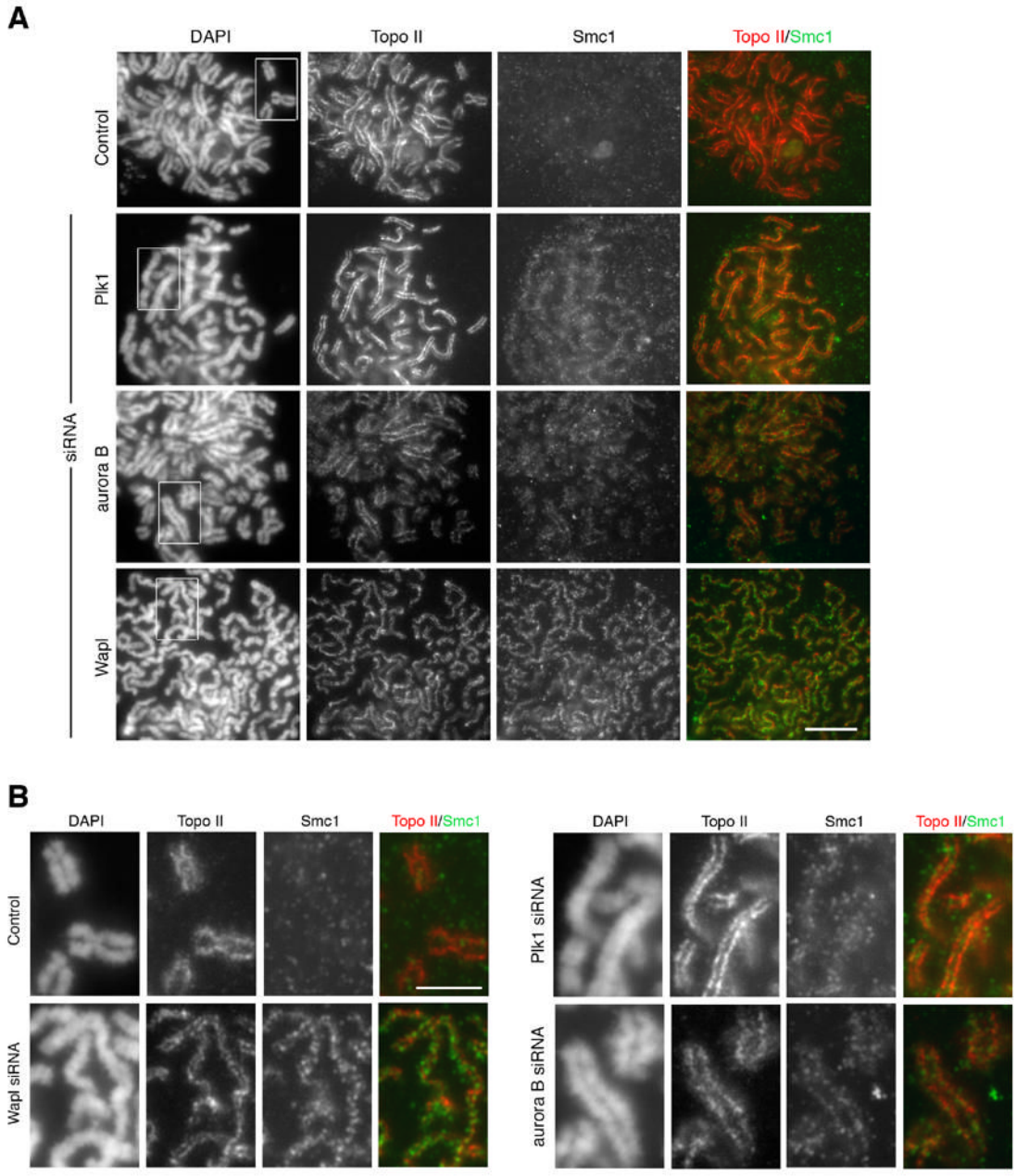

Figure 3.

Depletion of Wapl Produces Prometaphase-like Chromosomes with Poorly Resolved Sister Chromatids and a High Level of Cohesin. (A) HeLa cells were mock-treated (the first row) or treated with siRNA specific to Plk1 (the second row), aurora B (the third row) or Wapl (the fourth row). Chromosome spreads were prepared without colcemid treatment, and were stained with anti-topoisomerase II and anti-Smc1. The DNA was counterstained with DAPI. Bar, 10 μm. (B) Close-ups of chromosomes from the control and siRNA-treated cells. Areas indicated by the rectangles in (A) panels, are magnified here. Bar, 5 μm.

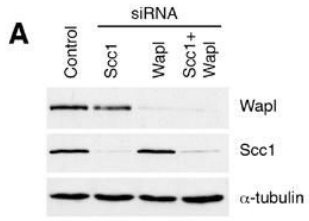

C

siRNA	Total cells		Chromosome spreads		
	Mitotic Index(%)	Abnormal mitotic cells (%)	Prometaphase like (%)	Metaphase like (%)	Premature separation (%)
Control	4.5	0	2.7	91.7	5.5
Scc1	13.5	90.5	0	0	100
Wapl	3.4	0	85.1	14.8	0
Scc1+Wapl	5.5	4.1	7.1	92.8	0

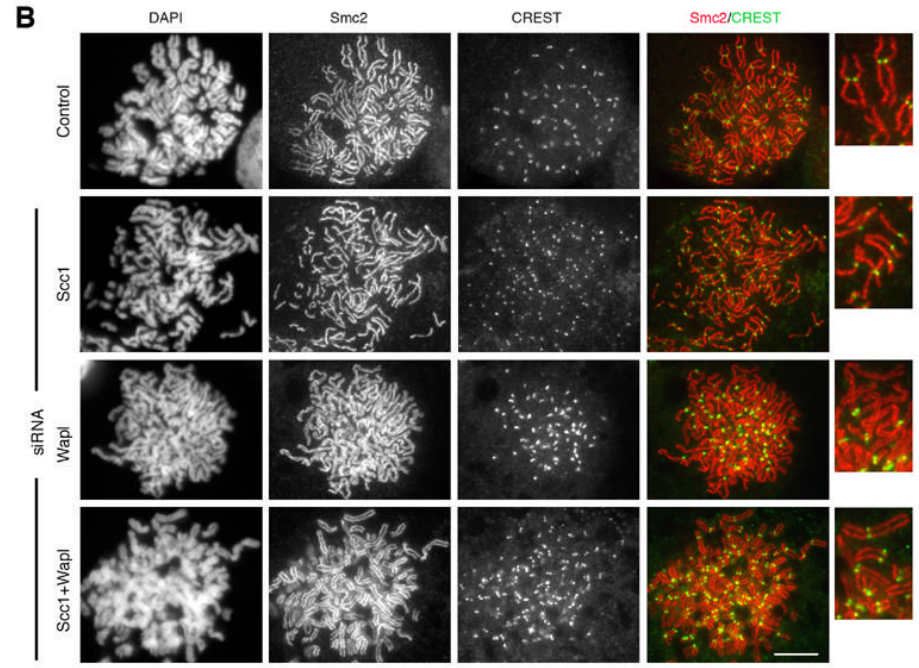

D

siRNA	Total cells		Chromosome spreads		
	Mitotic Index(%)	Abnormal mitotic cells (%)	Prometaphase like (%)	Metaphase like (%)	Premature separation (%)
Control	3.8	4.3	6.1	87.8	6.1
Wapl	3.6	0	62.2	37.8	0
Sgo1	24.2	100	0	2.2	97.7
Sgo1+Wapl	4.3	31.8	50.0	25.0	25.0

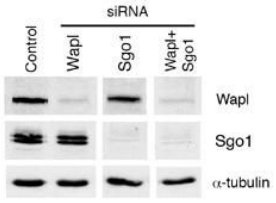

E

siRNA	Total cells		Chromosome spreads		
	Mitotic Index(%)	Abnormal mitotic cells (%)	Prometaphase like (%)	Metaphase like (%)	Premature separation (%)
Control	6.0	0	27.5	58.6	10.3
Wapl	4.4	0	100	0	0
Esco2	20.0	88.0	0	12.9	87.0
Wapl+Esco2	3.8	6.6	72.4	17.2	10.3

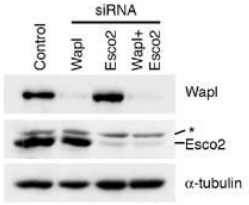

Figure 4.

Functional Interactions among Wapl, Cohesin and Cohesin Regulators. (A) HeLa cells were mock transfected (Control) or transfected with Scc1, Wapl, or Scc1 and Wapl siRNAs, and cell lysates were prepared and analyzed by immunoblotting analysis using the antibodies indicated. (B) Chromosome spreads were prepared (without colcemid treatment) from the control and siRNA-transfected cells, and stained with an anti-Smc2 antibody and CREST serum. Merged images are also shown on the right. Bar, 10 μm. (C) Quantification of mitotic parameters observed in the control and siRNA-treated cells. Abnormal mitotic cells include cells displaying chromosome misalignment and abnormal anaphase-like cells indicative of premature chromatid separation. (D) Quantification of mitotic defects and chromosome

phenotypes observed in control cells and cells transfected with siRNAs specific to Wapl, Sgo1, or Wapl+Sgo1 (left). The efficiency of depletion in each sample was assessed by immunoblotting (right). (E) A similar set of experiment was performed using siRNAs specific to Wapl, Esco2, and Wapl+Esco2, and analyzed as in (D). The asterisk above the Esco2 band indicates a non-specific band.

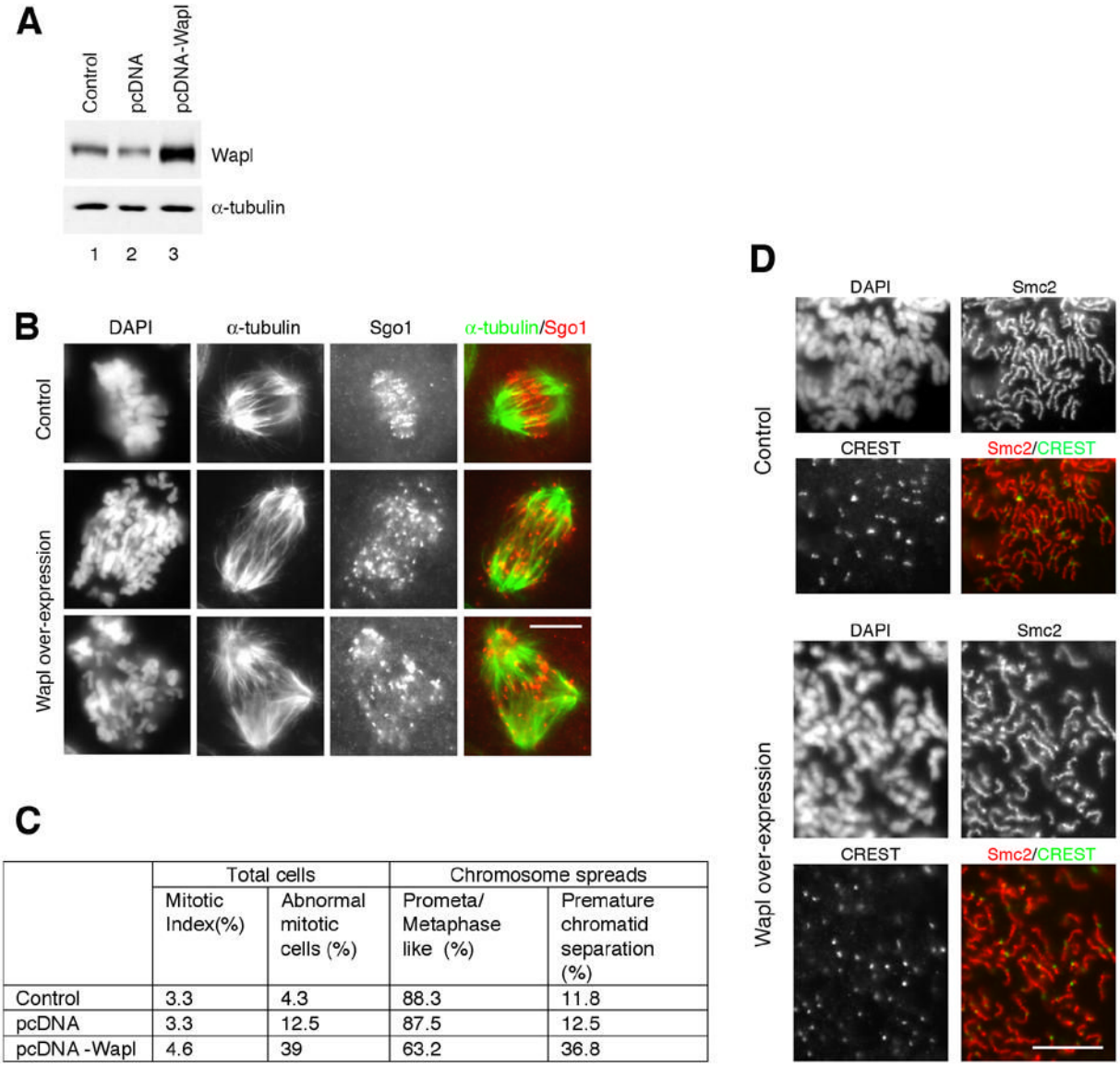

C

	Total cells		Chromosome spreads	
	Mitotic Index(%)	Abnormal mitotic cells (%)	Prometa/ Metaphase like (%)	Premature chromatid separation (%)
Control	3.3	4.3	88.3	11.8
pcDNA	3.3	12.5	87.5	12.5
pcDNA -Wapl	4.6	39	63.2	36.8

Figure 5.

Overexpression of Wapl Causes Segregation Defects Reminiscent of Those Found in Cohesin-deficient Cells. (A) 293T cells were transfected with a plasmid harboring Wapl cDNA under the control of the CMV promoter in pcDNA3.1 (lane 3) or with the corresponding empty vector (lane 2). Cell lysates were prepared 42 hr after transfection and analyzed by immunoblotting along with a lysate from untransfected cells (lane 1). (B) The control and Wapl cDNA-transfected cells were fixed and stained with antibodies against α-tubulin and Sgo1. The DNA was counterstained with DAPI. Shown are representative mitotic figures for each population of cells. Bar, 10 μm. (C) Quantitation of abnormalities observed in total cells (B) and in chromosome spreads (D). (D) Chromosome spreads were prepared from the control and Wapl cDNA-transfected cells, and stained with an antibody against Smc2 (a condensin subunit) and a CREST serum. The DNA was counterstained with DAPI. Bar, 10 μm.

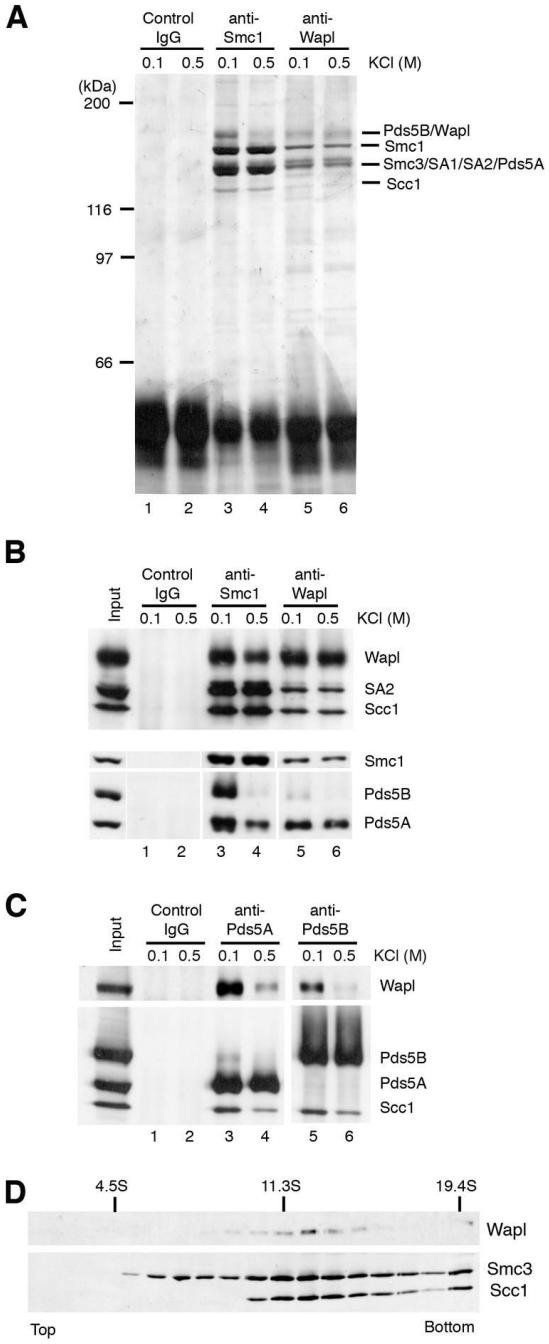

Figure 6.

Wapl Interacts with Cohesin in HeLa Cell Nuclear Extracts. (A&B) HeLa cell nuclear extracts were subjected to immunoprecipitations with control IgG (lanes 1 and 2), anti-Smc1 (lanes 3 and 4) or anti-Wapl (lanes 5 and 6). The precipitates were washed with a buffer containing 0.1 M KCl (lanes 1, 3 and 5) or 0.5 M KCl (lanes 2, 4 and 6), and analyzed by silver staining (A) or immunoblotting using the antibodies indicated (B). 5% of the input sample was loaded in the first lane (input) of panel (B). (C) The same extracts were used for immunoprecipitations using control IgG (lanes 1 and 2), anti-Pds5A (lanes 3 and 4) or anti-Pds5B (lanes 5 and 6). The precipitates and the input sample were analyzed as above. (D) A HeLa nuclear extract was loaded onto a 5–20% sucrose gradient and centrifuged at 36,000 rpm for 15 h in an SW50.1

rotor. Fractions were subjected to SDS-PAGE and analyzed by immunoblotting. The positions of three protein standards (BSA [4.5S], catalase [11.3S] and thyroglobulin [19.4S]) are indicated.

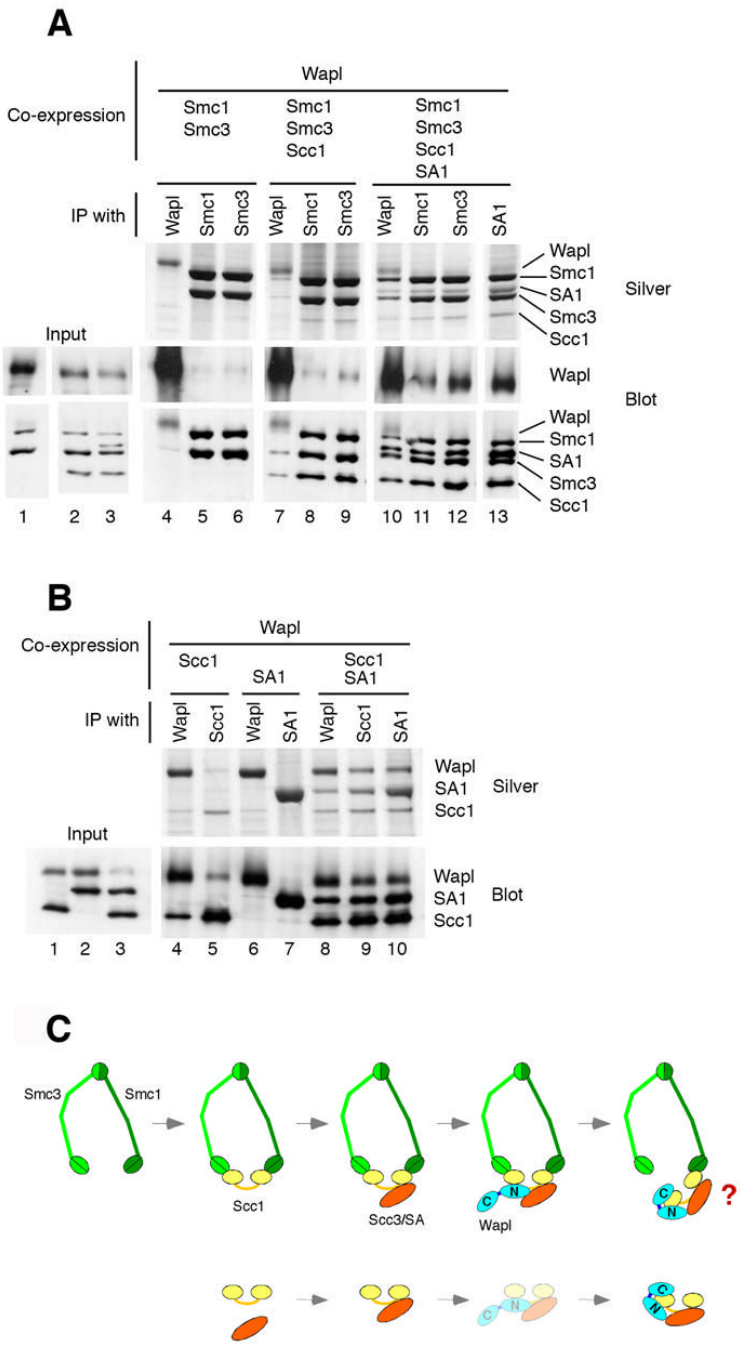

Figure 7.

In Vitro Reconstitution Reveals that Wapl Directly Associates with the Non-SMC Dimer of Cohesin. (A) Wapl was co-expressed in Sf9 cells with Smc1 and Smc3 (lanes 1, 4–6), Smc1, Smc3 and Scc1 (lanes 2, 7–9), or Smc1, Smc3, Scc1 and SA1 (lanes 3, 10–13). Cell lysates were prepared (lanes 1–3; input) and subjected to immunoprecipitations with the antibodies indicated (lanes 4–13). The precipitates were divided into two aliquots, resolved by SDS-PAGE, and analyzed by silver stain (Silver) and immunoblotting using the antibodies indicated (Blot). (B) Wapl was co-expressed in Sf9 cells with Scc1 alone (lanes 1, 4 and 5), SA1 alone (lanes 2, 6 and 7) or Scc1 and SA1 together (lanes 3, 8–10). Cell lysates were prepared (lanes 1–3; input) and reciprocal immunoprecipitations were performed using the antibodies indicated

(lanes 4–10). The precipitates were analyzed as described in (A). (C) A schematic diagram of the order of subunit interactions. Wapl can associate only with the holocomplex of cohesin or the Scc1-SA dimer. A hypothetical model for Wapl's action is shown at the right end of the upper panel.